Neutron Scattering of Hydrophobically Modified Poly(ethylene oxide) in Aqueous Solutions

Emmanuel Beaudoin,† Oleg Borisov,† Alain Lapp,‡ Laurent Billon,† Roger C. Hiorns,† and Jeanne François*,†

Laboratoire de Physico-chimie des Polymères, UMR 5067 UPPA/CNRS, Hélioparc, 2 Avenue du Président Angot, 64053 Pau, France, and Laboratoire Léon Brillouin, CEA Saclay, 91191 Gif-sur-Yvette, France

Received June 15, 2001; Revised Manuscript Received May 28, 2002

ABSTRACT: The structure of aqueous dispersions of hydrophobically end-capped poly(ethylene oxide) (PEOM) was investigated by small-angle neutron scattering. Two polymers, M16C16 and D32C16, with the same hydrophilic/hydrophobic balance, with either one or two *n*-hexadeca end groups and average molecular weights, *M*, 16 000 and 32 000 g mol^{-1}, respectively, were studied in heavy water. In addition, a sample of poly(ethylene oxide), $M = 35\,000$ g mol^{-1}, with deuterated *n*-octadecyl end groups was studied in heavy water and in a heavy water/water mixture (17.6% D_2O) to selectively match the PEO chain. In all the cases, the scattering curves were characterized by a main peak which revealed that the polymers were organized in micelles forming an organized liquid structure. In heavy water, the peak maximum scattered intensity, I_{max}, has a maximum at a concentration corresponding to micelle overlapping, and I_{max} increases with increasing temperature, at constant concentration. In a mixture containing 17.6% D_2O, I_{max} continuously increases with polymer concentration. This scattering behavior is interpreted on the basis of an analogy between micellar solutions and dilute and semidilute solutions of star-branched polymers.

Introduction

Associative polymers (AP) formed from hydrophilic poly(ethylene oxide), PEO, chains with one or two aliphatic end groups, α- or α,ω-modified PEO or PEOM, self-assemble in aqueous dispersions to form respectively micelles or "flowers".[1−4] PEO-based AP are particularly interesting as it is possible to prepare model samples with low molecular weight distributions and well-controlled degrees of functionalization[5,6] and also because solubility of PEO in water is easily tuned by varying temperature. Micellization occurs above a well-defined critical concentration, CAC, which is generally measured by fluorescence or light scattering.[5−10] At concentrations where micelles overlap, C_f*, an abrupt jump in viscosity is observed with the difunctionalized polymers, while the equivalent increase in viscosity of monofunctionalized polymer varies little from that of unmodified PEO.[11] Moreover, the association mechanism has been investigated by light scattering[9,10] and a model of closed association was proposed when only micelles are formed as in the case of α-PEOM.[10] When intermicellar bridges are formed, as in the case of α,ω-PEOM, two association steps were identified, the first being cooperative—a closed association—forming the "flower" like micelles and the second being more progressive—an open association—corresponding to "flower" association,[8−10] via formation of bridges.

While this paper deals with the structure of this type of AP in dispersions above the CAC, it has already been demonstrated by neutron[5,6] and X-ray[7] scattering that "flowers" of α,ω-PEOM are organized in a liquid order (Figure 1). In a series of experiments, we mainly studied the influence of polymer composition and concluded that the degree of order increases on decreasing the molecular weight of the PEO chains or increasing the length of the hydrophobic groups. The size and shape of the hydrophobic nanodomains have been studied in water/heavy water (82.4%/17.6% v/v) mixtures where the PEO chains are matched, and we concluded that the "flower" cores can be considered as spheres with radii increasing with increases in concentration while, at the same time, dependent upon the PEO chain length (for a same hydrophobic groups).

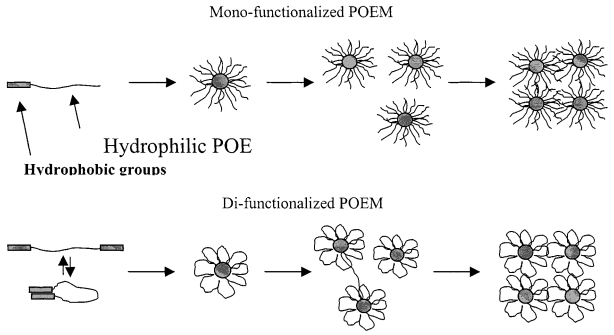

Figure 1. Schematic representation of the association of mono- and difunctionalized PEO.

This work is a systematic investigation of the scattering behavior of hydrophobically modified poly(ethylene oxide). As only α,ω-PEOM were previously investigated, we now compare in this paper the behavior of α-PEOM and α,ω-PEOM samples of the same hydrophilic/hydrophobic balance: the end groups are *n*-hexadeca aliphatic chains and the molecular weights of PEO chains are respectively 16 000 and 32 000 g mol^{-1}. The aim is to separate the effects of bridging (only in cases of α,ω-PEOM) and steric interactions (both α-PEOM and α,ω-PEOM) between micelles. Investigated are the influences of polymer concentration and temperature. A difunctionalized polymer with the same molecular weight ($M = 35\,000$ g mol^{-1}) but deuterated *n*-octadeca groups was also studied. It was studied in

* To whom correspondence should be sent.
† UMR 5067 UPPA/CNRS.
‡ CEA Saclay.

10.1021/ma011027l CCC: $22.00
Published on Web 08/15/2002

heavy water, where no part of the molecule is matched, and in a mixture of water/heavy water (17.6%). where PEO is matched. In the first part of this paper, we present the theoretical basis of the interpretation of the experimental results. The experimental setup and the preparation of the samples are described in the second part, while the experimental results and the discussion are presented in the third part of this paper.

Theory

Many attempts to model SANS curves of polymeric systems forming micelles have already been made.[11−17] Generally the systems studied were EO/PO copolymers, linear or branched. Mortensen[11] has considered micelles as hard spheres, without taking into account internal structure of the swollen PEO corona. More elaborated models were proposed in which scattered intensity was attributed to micelles consisting of several layers with a hard PO core surrounded by PEO layers with a differing degree of swelling.[16,17] It must be noted that, in the case of these copolymers, the PEO and PPO chains are considerably shorter than in our associative polymers for which the core is very small with respect to the corona. Moreover, experiments in solvents selectively matching PPO cores with PEO coronas have not been performed.

On the other hand, the literature provides theoretical calculations of the form factors of polymer stars to which micelles or flowers may be assimilated.[18−21] Several investigations of the scattering behavior of stars in dilute solutions have been published,[22−24] in which the interaction between the micelles (the structure factor) is neglected. When the correlations between stars become important, one has to introduce a structure factor, and several models may be used. Very often, the interaction potential of hard spheres is used[17−20,25,26] in the case of micellar systems. The true potential of soft spheres or polymer stars has been calculated, but it leads to a structure factor which is not a simple analytical expression.[27−29] In the dilute regime, it should be possible to obtain the structure factor from the scattering curves by dividing the total scattering intensity, $I(q)$, by the form factor, if it is known.[29] The method is limited to stars with a well-determined number of branches and can only be used in the dilute regime since, in semidilute solutions, the star conformation is expected to change with concentration.

Therefore in our analysis we utilize the combined model of the micellar solution: this model includes only experimentally measurable parameters, i.e., the aggregation number and the hydrodynamic radius of the micellar corona, and enables us to obtain analytical expressions for the scattering intensity as a function of concentration. For the description of scattering from the micellar coronas (when PEO chains are not matched, the study in heavy water) we utilize the star-polymer model, thus taking into account explicitly the intrinsic conformational structure of the PEO chains in the coronas. The structure factor which is due to the interaction between crowding coronas of different micelles is calculated, however, on the basis of the model of equivalent hard spheres, i.e., depending on concentration of micelles and on the effective interaction radius; as we discuss below, this effective interaction radius appears to be a function of the polymer concentration in the solution.

The starting point is the general equation for scattering:

$$\Delta I(q) = \frac{(\Delta b)^2}{N_A} C \overline{M_w} N_{ag} P(q) S(q) \quad (1)$$

Here C is the concentration of polymers (g/cm^3), M_w is the weight average molecular weight (g/mol), $N_A = 6.022 \times 10^{23}$ mol^{-1} is the Avogadro number, N_{ag} is the aggregation number (number of the polymer chains associated into one micelle), $\Delta b = \Delta\rho^* v_{sp}$ is the contrast length in cm/g ($\Delta\rho$ is the contrast factor, and v_{sp} is the specific volume of the scattering species). $P(q)$ and $S(q)$ are the form and the structure factors, respectively.

Two different scattering species are present in our polymers: the aliphatic end groups and the PEO chains. In a solvent where no part of the polymer is matched, the scattered intensity contains three different terms where the indices 1, 2, and 12 refer to the intra- and intercorrelations between the same scattering species 1 and 2 and to the crossed correlations between scattering species 1 and 2, respectively. In our subsequent discussion we ascribe index 1 to the aliphatic chains and index 2 to the PEO chains.

$$\Delta I = \frac{(\Delta b_1)^2}{N_A} C_1 \overline{M_{w1}} N_{ag} P_1(q) S_1(q) + \frac{(\Delta b_2)^2}{N_A} C_2 \overline{M_{w2}} N_{ag} P_2(q)\, S_2(q) + X \quad (2)$$

Here X is a crossed term proportional to the product to $\Delta b_1 \Delta b_2 \cdot C_1 C_2$.

In a solvent where PEO chains are matched ($\Delta\rho_2 = 0$), the second and third terms vanish. When the solvent is heavy water, the value of $\Delta b_2^2 C_2$ is more than 100 times higher than $\Delta b_1^2 C_1$ or $\Delta b_1 \Delta b_2 \cdot C_1 C_2$ and one can consider only the second term.

Our experimental results clearly show that qualitative changes in scattering phenomenon are observed when C exceeds the critical concentration of micelle or flower overlap, C_f^*. Therefore, we shall consider successively the dilute regime ($C < C_f^*$) and the semidilute regime ($C > C_f^*$).

(1) Dilute Regime. (a) Structure Factor. The structure factor $S(q)$ in dilute solution of micelles is determined by the interaction between swollen PEO coronas of the micelles. Therefore, it is the same in both solvents where PEO chains are matched or not, $S_1(q) = S_2(q) = S(q)$. The general expression for $S(q)$ is[30]

$$S(q) = \left[1 + N_m \int_0^\infty g(r) \frac{\sin qr}{qr} 4\pi r^2 dr\right] = 1 + N_m g(q) \quad (3)$$

where N_m is the number of micelles/unit volume and $g(q)$ is the Fourier transform of the pair correlation function $g(r)$. N_m can be calculated from the aggregation number, if known:

$$N_m = \frac{N_A C}{\overline{M_w} N_{ag}} \quad (4)$$

An analytical expression for $g(q)$ has been calculated for monodisperse solutions of hard spheres of radius R within the Percus−Yevick approximation and leads to the following expression for the structure factor:

$$S(q) = \left[1 + 24\Phi \frac{G(2qR,\Phi)}{2qR}\right]^{-1} \quad (5)$$

Here $G(2u,\Phi)$ is a function of $u \equiv qR$ and volume fraction Φ, occupied by spheres,

$$G(2u,\Phi) = (\alpha(\Phi)/4u^2)[\sin(2u) - 2u\cos(2u)]$$

$$+ (\beta(\Phi)/8u^3)[4u\sin(2u) + (2 - 4u^2)\cos(2u) - 2]$$

$$+ (\gamma(\Phi)/32u^5)[-16u^4\cos(2u) + 4[(12u^2 - 6)\cos(2u) + (8u^3 - 12u)\sin(2u) + 6]] \quad (6)$$

and α, β, and γ are functions of the volume fraction Φ:

$$\alpha(\Phi) = (1 + 2(\Phi))^2/(1 - \Phi)^4$$

$$\beta(\Phi) = -6\Phi(1 + \Phi/2)^2/(1 - \Phi)^4$$

$$\gamma(\Phi) = (\Phi/2)(1 + 2\Phi)^2/(1 - \Phi)^4 \quad (7)$$

There is only one adjustable parameter, the radius R, since the volume fraction Φ is given by

$$\Phi = N_m V = \frac{N_A C}{M_w N_{ag}} \frac{4}{3}\pi R^3 \quad (8)$$

For true hard spheres, R corresponds exactly to the sphere radius; in fact, in this work we assimilate micelles to hard spheres for calculation of $S(q)$. Therefore, we replace R by the effective interaction radius R_{hs} in eqs 5−8.

(b) PEO Matched Chains. In the case when the PEO chains are "invisible" ($\Delta b_2 = 0$) and do not contribute to the scattering intensity, the equation for the scattering intensity assumes the most simple form:

$$\Delta I(q) = \frac{(\Delta b_1)^2}{N_A} C \frac{M_a^2}{M_w} N_{ag} P(q)\, S(q) \quad (9)$$

Here Δb_1 and M_a are the contrast length and the molecular weight of the aliphatic chains, respectively. $P(q)$ is the form factor of the micellar core, and $S(q)$ is the structure factor which accounts for the interactions between ("invisible") micellar coronas. As the core can be assimilated to a uniform sphere of radius R_c, we can utilize the classical form factor of uniform spheres:[30]

$$P(q) = \left[\frac{3}{(qR_c)^3}(\sin qR_c - qR_c \cos qR_c)\right]^2 \quad (10)$$

(c) PEO Unmatched Chains. In heavy water, the dominant contribution to the overall scattering intensity is due to the coronas of micelles. According to the approach of Auvray−de Gennes,[31] the scattering intensity from the dilute solution of starlike micelles can be decomposed into two contributions. The first term originates from correlated fluctuations in a local concentration of micelles and is proportional to the product of the form factor of a micelle (calculated by taking into account the average radial distribution of the monomer density in the micellar corona) and the structure factor which accounts for the interaction between micelles. The second term is due to correlated fluctuations of the monomer density inside the micellar coronas. Because the micellar corona locally is equivalent to the semidilute polymer solution, the second term has a Lorentzian form. Altogether, the expression for the scattering intensity yields

$$\Delta I(q) = \frac{(\Delta b_2)^2}{N_A} C \overline{M_w} N_{ag} \left(\alpha P(q)\, S(q) + \beta \frac{1}{1 + q^2\xi^2}\right) \quad (11)$$

where ξ is an appropriate correlation length (the average blob size) in the micellar corona.

Equation 11 is expected to provide an interpolation for $I(q)$ in wide range of q from $q \geq 0$ up to $q \leq \xi^{-1}$. The choice of the weight factors $\alpha = (N_{ag} - 1)/N_{ag}$ and $\beta = 1/N_{ag}$ in eq 11 ensures that, in the infinitely dilute solution, $C \to 0$, in the limit $q = 0$ (when both $S(q) = 1$ and $P(q) = 1$) the overall intensity extrapolates to

$$\Delta I(q = 0) = \frac{(\Delta b_2)^2}{N_A} C \overline{M_w} N_{ag} \quad (12)$$

while the contribution of the second term describing local monomer density fluctuations scales proportionally to the molecular mass of a single chain. This type of decomposition of the scattering intensity has been first suggested for a dilute solution of starlike micelles in refs 32 and 33 and in the more particular form of eq 12 in refs 34 and 35.

(d) Form Factor of the Corona. The model used to calculate the form factor of the micellar corona is represented in Figure 2. As long as the radius of the core is negligible in comparison to that of the corona, the latter can be assimilated to a starlike polymer[36,37] with N_{ag} branches and can be presented as an array of concentric shell of close-packed blobs. The blob size, $\xi(r)$, increases with the distance r from the center of the micelles as $\xi(r) \cong r\, N_{ag}^{-1/2}$. The polymer concentration in the corona decreases with r as $C(r) \cong N_{ag}^{(1-\nu)/2} r^{(1-3\nu)/\nu}$, where ν is the Flory exponent ($\nu = 3/5$ or $1/2$ under good or Θ-solvent conditions, respectively).

Then the form factor of a starlike micelle has the form[21]

$$P(q) = \left[\frac{4\pi\int_0^R C(r)\frac{\sin(qr)}{qr} r^2\, dr}{4\pi\int_0^R C(r) r^2\, dr}\right]^2 = \left[F\left(\frac{1}{2\nu}, \left(\frac{3}{2}, 1 + \frac{1}{2\nu}\right), -\frac{q^2R^2}{4}\right)\right]^2 \quad (13)$$

where $F(\{a\},\{b\},x)$ is the generalized hypergeometric function and we have neglected the core size setting the lower limit of integration equal to zero. R is the cutoff length of the concentration profile (determined by the normalization of $C(r)$) which can be roughly assimilated to the hydrodynamic radius of the corona. In Θ solvent, $C(r) \sim 1/r$, eq 13 is reduced to

$$P(q) = \left[\frac{2}{(qR)^2}(1 - \cos(qR))\right]^2 \quad (14)$$

This expression is applicable at high temperatures close to the LCST. The $1/r^{4/3}$ profile should apply at lower temperatures since water is a good solvent for PEO. Remarkably the shape of the form factor $P(q)$ is relatively insensitive to the particular value of the exponent describing the radial decay of the polymer density in the micellar corona. Therefore, we utilized for the fit of our experimental data the analytical expression for the form factor, $P(q)$, given by eq 14.

We remark that the power-law dependence for the polymer concentration on r well describes the central

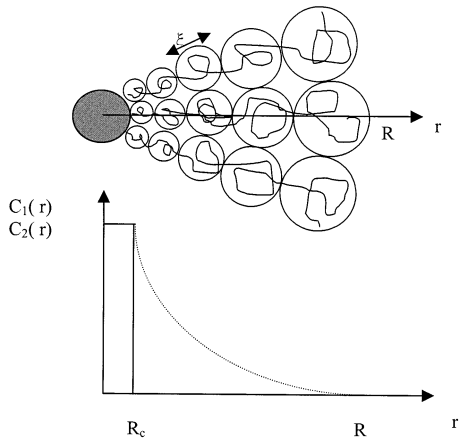

Figure 2. Daoud−Cotton model for starlike polymer micelles.

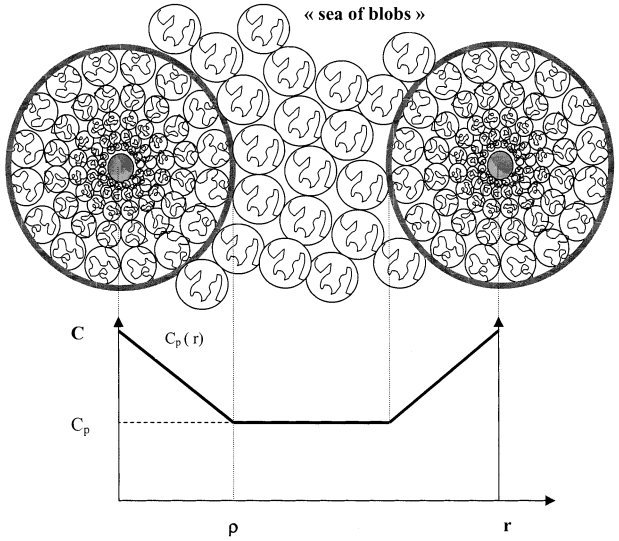

Figure 3. Schematic representation of semidilute solutions of starlike polymer micelles. The "sea of blobs" and internal unperturbed regions of coronas are depicted.

regions of the micelle corona but is violated near the edge of the corona, where the polymer density vanishes smoothly; the polymer density profile in this external region acquires approximately a parabolic shape.[38] In our calculations of the form factor we do not take this deviation into account explicitly though it can affect the value of the apparent radius of the corona providing the best fit of the scattering curves.

(2) Semidilute Regime. (a) PEO Unmatched Chains. We will consider at first the case where PEO chains were not matched and thus contribute mainly to the scattered intensity.

The semidilute solution of the starlike micelles can be schematized as in Figure 3, where the overlapped regions of the coronas constitute semidilute polymer solution which can be viewed as the "sea of blobs" of constant size ξ, while within the radius ρ an unperturbed structure of the corona equivalent to that in the dilute regime is preserved.[36,39] We shall refer to these unperturbed internal regions as "depleted micelles" which are embedded in the "sea of blobs". The monomer concentration profile is also schematically presented in Figure 3. The concentration inside the "sea of blobs" is uniform, and we denote it as C_b. The concentration in the unperturbed internal regions of the micellar coronas decreases as a function of the distance r from the center of the micelles reaching the value of C_b at the edge of the unperturbed part, i.e., at $r = \rho$.

Following ref 40, we shall assume that the scattering intensity, $\Delta I(q) = \Delta I_s(q) + \Delta I_b(q)$, can still be decomposed into two contributions. The first one (ΔI_s) describes scattering due to correlated fluctuations in the positions of the unperturbed internal regions of the micellar coronas, whose radius ρ decreases with increases in concentration; the second contribution (ΔI_b) is due to local fluctuations in the concentration of monomers both in the "sea of blobs" and inside unperturbed internal regions of the micellar coronas.

(i) Evaluation of ΔI_s. The radius ρ of the unperturbed internal region of the coronas depends on the overlap degree of the micelles, i.e., on C/C_f^*, and can be found from the condition $C(\rho) = C_b$, which leads to

$$\frac{1}{3\nu} r_c^{\,1-3\nu/\nu}\left[1 - \frac{3\nu - 1}{3\nu} r_c^{\,1/\nu}\right]^{-1} = \frac{C}{C_f^*} \qquad (15)$$

where r_c is the ratio between $\rho(C)$ and the radius of the micelle in the dilute regime, R:

$$r_c = \frac{\rho(C)}{R} \qquad (16)$$

As follows from eq 15, $r_c = 1$ (i.e. $\rho = R$) at $C = C_f^*$. In Θ solvent, $\nu = 1/2$, eq 15 reduces to

$$r_c^{\,3} - 3r_c + \frac{2}{C/C_f^*} = 0 \qquad (17)$$

By using this expression, it is easy to calculate r_c if the ratio C/C_f^* is known.

For the calculation of the form factor of the depleted micelles we have to take into account that (1) the central-symmetrical monomer density profile $C(r)$ extends up to $\rho(C)$ and (2) the background concentration C_b has to be subtracted from $C(r)$, which corresponds to the effective reduction of the contrast for depleted micelles embedded in the semidilute polymer solution (the "sea of blobs") of concentration C_b. As a result, one gets

$$P(q) = \left[\frac{4\pi\int_0^{\rho(c)} \frac{\sin(qr)}{qr}(C(r) - C_b) r^2\,dr}{4\pi\int_0^{\rho(c)} (C(r) - C_b) r^2\,dr}\right]^2 \qquad (18)$$

However, due to the power-law dependence of the polymer density on r, we have a simple relation between the polymer density $C(r)$ inside the unperturbed region of the micellar corona and the density C_b in the sea of blobs

$$\frac{C(r)}{C_b} = \left(\frac{r}{\rho}\right)^{(1-3\nu)/\nu} \qquad (19)$$

and eq 18 becomes

$$P(q) = \left[\frac{\int_0^{\rho(c)} \frac{\sin(qr)}{qr}\left(\left(\frac{r}{\rho}\right)^{(1-3\nu)/\nu} - 1\right) r^2\,dr}{\int_0^{\rho(c)} \left(\left(\frac{r}{\rho}\right)^{(1-3\nu)/\nu} - 1\right) r^2\,dr}\right]^2 \qquad (20)$$

Finally, the expression for $\Delta I_s(q)$ reads

$$\Delta I_s(q) = \frac{\Delta b_2^{\,2}}{N_A^{\,2}} N_m \left[\frac{3\nu - 1}{\nu}(\overline{M_w} N_{ag})\left(\frac{\rho}{R}\right)^{1/\nu}\right]^2 \left[\frac{\int_0^{\rho(c)} \frac{\sin(qr)}{qr}\left(\left(\frac{r}{\rho}\right)^{(1-3\nu)/\nu} - 1\right) r^2\, dr}{\int_0^{\rho(c)}\left(\left(\frac{r}{\rho}\right)^{(1-3\nu)/\nu} - 1\right) r^2\, dr}\right]^2 S(q) \quad (21)$$

and for $\nu = 1/2$ one gets

$$\Delta I_s(q) = \frac{\Delta b_2^{\,2}}{N_A^{\,2}} N_m \left[(\overline{M_w} N_{ag})\left(\frac{\rho}{R}\right)^2\right]^2 \left[\frac{6(q\rho - \sin(q\rho))}{q^3\rho^3}\right]^2 S(q) \quad (22)$$

where the structure factor $S(q)$ depends on the effective interaction potential between the depleted micelles. For the calculation of $S(q)$ we use again the equivalent hard sphere model, similarly to the case of dilute solution. However, in semidilute solutions, the effective interaction radius is expected to depend explicitly on the polymer concentration (i.e., on the degree of overlapping of micellar coronas). The radius $\rho(C)$ of the unperturbed internal regions of micelles may serve as a lower estimate for the interaction radius. As has been demonstrated in ref 39, the interpenetration of the coronas progressively increases upon an increase in concentration above C_f^*. In a wide range of concentrations corresponding to the semidilute solution, the PEO chains in the corona remain extended in the radial direction and, as a result, the degree of interpenetration of the coronas of different micelles remains weak. Therefore we expect that the effective interaction radius between depleted micelles in the semidilute solution is smaller than that in dilute solution but larger than $\rho(C)$.

(ii) Evaluation of $\Delta I_b(q)$. The contribution $\Delta I_b(q)$ to the scattered intensity is expressed similarly to the case of a semidilute polymer solution as a function of the average concentration of monomers/unit volume $\overline{C}$.

$$\Delta I_b(q) = K_I \overline{C}^2 (\Delta b_2)^2 \frac{\xi^3}{1 + q^2\xi^2} \quad (23)$$

where K_I is a numerical prefactor and ξ is the (average) correlation length which depends on $\overline{C}$. For the semidilute solution of linear chains, K_I has been calculated in ref 41 within the RPA and is equal to $2^{9/4}\pi^{3/4}$. By the approximation leading to eq 23, we effectively smear out locally higher monomer concentration (and, as a result, locally smaller correlation length) in the internal unperturbed regions of micelles. We expect that due to the power-law monomer density profiles inside the depleted micelles, this approximation affects only the numerical prefactor in the expression for ΔI_b. Moreover, at sufficiently high concentration, the contribution of the depleted micelles to the overall solution concentration and to $\Delta I_b(q)$ becomes negligible and $\overline{C}$ approaches C_b.

(iii) Total Scattered Intensity for Semidilute Solutions. Finally, the total intensity is the sum of eqs 22 and 23 and yields

$$\Delta I(q) = \frac{\Delta b_2^{\,2}}{N_A^{\,2}} N_m \left[(\overline{M_w} N_{ag})\left(\frac{\rho}{R}\right)^2\right]^2 \left[\frac{6(q\rho - \sin(q\rho))}{q^3\rho^3}\right]^2 S(q) + K_I \overline{C}^2 (\Delta b_2)^2 \frac{\xi^3}{1 + q^2\xi^2} \quad (24)$$

When concentration increases, the contribution of the first term—characterized by a peak resulting from $S(q)$—becomes negligible due to decreasing size and number of monomers in the unperturbed regions of the coronas. Then the scattered intensity is dominated by the second term, which describes scattering due to local monomer density fluctuation, just as in conventional semidilute solution contribution, and does not exhibit any peak. Clearly, at sufficiently high concentrations the main contribution to the latter term is that from the "sea of blobs". This qualitatively explains the disappearance of the scattering peak in the neutron scattering experiments performed in pure heavy water in which scattering is mainly due to PEO chains.

(b) PEO Matched Chains. If one considers now the case where PEO chains are matched and the contribution to the scattered intensity is that of the micelle core only, one can use the same eq 9 for the scattering intensity with the same uniform sphere form factor of the cores as in dilute solution, eq 10. We remark, however, that the aggregation number N_{ag} and, as a result, the core radius R_c in the semidilute regime are expected to be weakly increasing functions of concentration. The structure factor $S(q)$ accounts now for the interaction between partially overlapped and partially interpenetrating coronas and must be the same as in eq 24, if we compare the two types of experiments at the same concentration. On other words, the value of the effective radius of interaction R_{hs} must be the same.

Finally, the scattered intensity by the cores $\Delta I_c(q)$ is given by

$$\Delta I_c(q) = \frac{\Delta b_1^{\,2}}{N_A} C N_{ag} \frac{M_a^{\,2}}{\overline{M_w}} \left[\frac{3}{(qR_c)^3}(\sin qR_c - qR_c \cos qR_c)\right]^2 S(q) \quad (25)$$

Figures 4 and 5 show the evolution of the scattering intensities calculated from eqs 25 and 24, respectively, upon an increase in the polymer concentration. When the PEO chains are not matched (eq 24, Figure 5), the peak in the scattering intensity monotonically decreases with increasing concentration. On the contrary, when the PEO chains are matched (eq 25, Figure 4), the model predicts a continuous increase of the scattering peak as C increases.

Experimental Section

(1) Materials. (a) Preparation of Hydrophobically End-Capped PEO. (i) α,ω-Functionalized PEO (D32C16)**.** D32C16 was synthesized according to a method which differs slightly from that given by Kaczmarski and Glass.[42]

Hexadecyl isocyanate was reacted with the hydroxyl chain ends of α,ω-hydroxylated PEO (Fluka) in the presence of 1,4-diazabicyclo[2.2.2]octane, DABCO, according to the following experimental conditions.[10] A 30 g amount of α,ω-hydroxylated PEO was purified by dissolving in toluene and precipitating in ether and was then dried under vacuum. The reaction vessel was dried and kept under nitrogen before and during use to

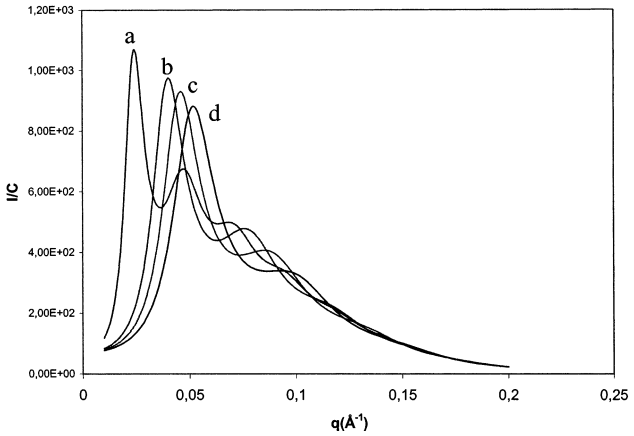

Figure 4. Scattered intensity reduced by the concentration calculated form eq 25, for matched PEO chains. The core radius was considered as independent of C: $R_c = 30$ Å. The interaction radius $R_h = R_{h0}(C^*/C)^{1/3}$. Curves a−d correspond respectively to polymer concentrations 0.05, 0.1, 0.2, and 0.5 g mL^{-1}.

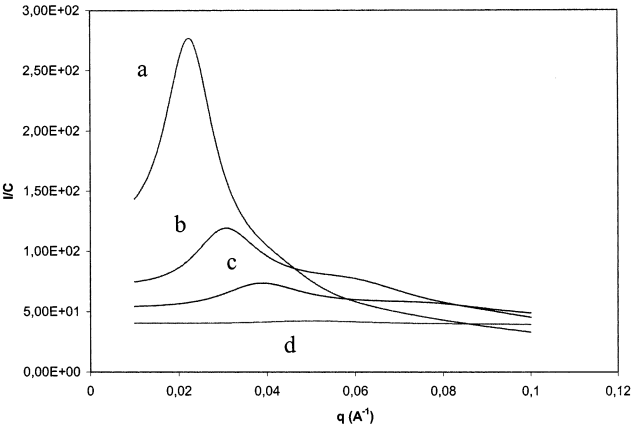

Figure 5. Scattered intensity reduced by the concentration calculated form eq 24, for unmatched PEO chains. The interaction radius is $R_h = R_{h0}(C^*/C)^{1/3}$, and the screening length ξ is calculated from the empirical law $\xi = 1.73C^{-0.68}$ determined by neutron scattering experiments on unmodified PEO of molecular weight 32 000.[35] Curves a−d correspond respectively to polymer concentrations 0.05, 0.1, 0.2, and 0.5 g mL^{-1}.

eliminate traces of water, which react with the isocyanate. Toluene (90 mL) used as solvent was heated at 80 °C over sodium prior to being cryodistilled into a 500 mL three-necked flask. PEO was introduced under nitrogen, and the mixture was heated to 60 °C until the PEO completely dissolved. DABCO (1% w/w with respect to the polymer) and an excess of hexadecyl isocyanate ($n = 3.8 \times 10^{-3}$ mol, 200% with respect to the PEO chain ends) were introduced. The reaction medium was maintained at 60 °C for 240 h to obtain complete functionalization. The hot reaction mixture was then filtered so as to eliminate reaction byproducts (urea) and diluted in toluene to 10% w/w. The resultant polymer was precipitated in ether and recrystallized twice from toluene.

The weight average molecular weight of the PEO precursor (N32) was determined by UV spectroscopy[10,43] and static light scattering, SLS. It was thereby found that $\overline{M}_w = 32\,000$. The molecular weight distribution, or polydispersity index, was measured by size exclusion chromatography: $\overline{M}_w/\overline{M}_n \approx 1.02$. N32 was also studied by neutron scattering experiments, and since no indication of degradation occurred during the chemical modification of PEO,[43] we will consider that $\overline{M}_w$ of D32C16 is also 32 000 g mol^{-1}.

(ii) Deuterated α,ω-Functionalized PEO (D35CD18). D35CD18 was obtained via the Williamson reaction of a deuterated octadecyl bromide on metalated PEO (obtained by modification of the hydroxyl end groups of PEO with biphenyl methyl potassium[6]).

The average molecular weight of the PEO precursor was determined by UV spectroscopy[10,43] and SLS: $\overline{M}_w = 35\,000$ g mol^{-1}. The index of polydispersity was measured by size exclusion chromatography: $\overline{M}_w/\overline{M}_n \approx 1.01$.

(iii) α-Functionalized PEO (M16C16). Remark: By using the same type of reaction on commercial samples as described above, it is possible to prepare only α-methylated, ω-hexadedylated PEO starting from α-methylated, ω-hydroxylated PEO (Me-PEO-OH). No Me-PEO-OH is commercially available with a molecular weight $\overline{M}_w = 16\,000$ g mol^{-1}, half of that of D32C16. Moreover, for the mono(hexadeca) end-capped PEO, it seemed better to have a polar −OH function at the other chain end instead of a hydrophobic methyl group.

It was thought that the most effective and least expensive route to poly(ethylene oxide) mono(hexadecyl ether) would be via the anionic polymerization of ethylene oxide using the initiator potassium hexadecyl oxide. The reaction could then be terminated with HCl, thus giving rise to the −OH chain end.

THF and toluene were distilled over their respective drying agents under predried nitrogen prior to use. The preparation of potassium hexadecyloxide was performed under predried nitrogen. The polymerization of ethylene oxide was performed using standard high-vacuum techniques.[44] Ethylene oxide was distilled under vacuum into break-seals of predetermined size; 1-hexadecanol, acidified methanol, and 18-crown-6 were also transferred into break-seals of predetermined size and sealed under high vacuum. Methanol, hydrochloric acid (37% solution in water) and 18-crown-6 were used as received. All chemicals were supplied by Aldrich.

(iv) Synthesis of Potassium Hexadecyl Oxide. Into a previously flame-dried and nitrogen-flushed Schlenk tube was placed excess potassium (1 g, 0.026 mol) and THF (100 mL). 1-Hexadecanol (0.25 g, 1.03×10^{-3} mol) was added and dissolved into the THF at room temperature. A white precipitate of potassium hexadecyl oxide slowly formed. After 18 h of stirring, the precipitate was left to settle, and the THF was removed with a syringe. The excess solid lumps of potassium were carefully removed with tweezers. Vacuum drying of the deposit over 18 h left a fine white powder (yield near 100%).

(v) Synthesis of Poly(ethylene oxide) Hexadecyl Ether. A 250 mL reactor fitted with a magnetic stirring bar, magnetic breakers, and break-seals containing ethylene oxide (13.6 mL, 12 g, 0.272 mol), potassium hexadecyl oxide (0.160 g, 5.70×10^{-4} mol), excess 18-crown-6 (0.3 g, 1.14×10^{-3} mol), and acidified methanol (2 mL) was evacuated and flame dried. Once THF (200 mL) was distilled into the vessel, it was sealed under high vacuum. Potassium hexadecyl oxide and 18-crown-6 were introduced and dissolved into the THF with stirring at 70 °C for 36 h. The solution was then cooled to 30 °C, and the ethylene oxide was introduced (*extreme care: the ethylene oxide was first frozen with by applying liquid nitrogen so that when the seal was broken, a rapid expansion of ethylene oxide—which would rupture the vessel—could not occur*). For the first 24 h of the polymerization the solution was stirred at 50 °C, after which the solution was stirred for 178 h at 70 °C. Addition of acidified methanol at room temperature caused a visible increase in the solution viscosity.

The polymer was precipitated twice from THF (200 mL) into diethyl ether (800 mL). The resulting fine white powder was collected by centrifuge and dried under vacuum at room temperature for 72 h to yield 10.9 g (91%).

(b) Characterization of Hydrophobically End-Capped PEO. (i) ^{1}H NMR. Samples were dissolved in a 50/50 mixture of $CDCl_3$ and DMSO and filtered prior to characterization. ^{1}H (400 MHz) NMR spectra were recorded on a Bruker AM-400 spectrometer. Residual hydrogen in deuterated chloroform was used to reference ^{1}H shifts. NMR can be used to determine the degree of functionalization and the average molecular weight of the polymer.

Characterization of M16C16 by ^{1}H NMR indicated, by integration, that there was the expected 3/1 ratio of methyl (0.8 ppm) to hydroxy (4.4 ppm) protons of the polymer end groups. The relative ratio of end groups to ethylene protons (3.5 ppm) indicated the polymer to have $\overline{M}_n$ of around 15 500 g mol^{-1}.

The degree of functionalization, τ, of D32C16 was indicated by ^{1}H NMR by using a internal probe (hexamethylcyclotrisiloxane)[6,11] of the main PEO chain: $\tau = 100\%$.

(ii) Size-Exclusion Chromatography. Molecular weights of M16C16 were obtained relative to polystyrene standards using size exclusion chromatography, SEC, equipment supplied by Waters. Determinations were carried out at 40 °C using a bank of 4 columns (HR 0.5, 2, 4, and 6) of 300 mm × 5 μm Styragel with an ERC INC 7515A refractive index, RI, detector. THF was used as eluent at a flow rate of 1.0 mL min^{-1} using a Waters 2690 pump.

GPC analysis indicated that the polymer's mass was higher than that found by NMR ($\overline{M}_n = 20\,640$, $\overline{M}_w/\overline{M}_w = 1.06$). The discrepancy between the results of the ^{1}H NMR and SEC characterizations may be explained by the calibration of the SEC being relative to polystyrene and not poly(ethylene oxide) standards thus introducing a large error.

(2) Small-Angle Neutron Scattering (Sans). SANS experiments were performed on PAXY spectrometer at Léon Brillouin Laboratory (LLB, Paxi instrument, CEA, Saclay, France) and at Laue Langevin Institut (Ill Grenoble, D11 intrument). Scattering ranges covered were $0.003 < q$ (Å^{-1}) < 0.22 and $0.018 < q$ (Å^{-1}) < 0.15, respectively. The temperature was varied between 5 and 70 °C.

The scattered intensity $I(q)$ for a solution or solvent is given by

$$I(q) = \frac{((I_s/(eT_s)) - (I_{cv}/(eT_{cv})))}{((I_{water}/(eT_{water})) - (I_{cv}/(eT_{cv})))}\left(\frac{d\Sigma}{d\Omega}\right)_{water} \quad (26)$$

where $(d\Sigma/d\Omega)_{water}$ is the effective cross section of water, e is the cell thickness, I_s, I_{cv}, and I_{water} are the scattered intensities of the sample, the empty cell, and water, respectively (from which the electronic noise measured with cadmium was subtracted), and T_s, T_{cv}, and T_{water} are the transmitted intensities of the sample, the empty cell, and water, respectively.

The coherent contribution ΔI of a solute can be calculated from the intensity scattered by the solution $I(q)_{solution}$, that scattered by pure solvent $I(q)_{solvent}$, the solute volume fraction Φ_p, and the incoherent contribution of the solute I^{inc}.

$$\Delta I = I(q)_{solution} - (1 - \Phi_p)I(q)_{solvent} - \Phi_p I^{inc}(q) \quad (27)$$

The incoherent contribution of the PEO chain was determined with a solution of pure PEO in water/heavy water mixture where its coherent contribution was matched (17.6% D_2O).

The contrast factor is

$$\Delta\rho^2 = (\rho_{sol} - \rho_{solvent})^2 \quad (28)$$

where ρ_{sol} and $\rho_{solvent}$ are the length scattering densities of the part of the polymer considered (PEO chains or aliphatic end groups) and of the solvent (heavy water or mixtures of water and heavy water), respectively.

Samples M16C16 and D32C16 were studied in heavy water. Sample D35CD18 (with deuterated end groups) was studied in heavy water where the major contribution to scattering is PEO chains. There was also studied a mixture of water/heavy water (82.4/17.6% v/v) where PEO is perfectly matched at 25 °C. Due to the change in the molar volume of PEO, the concentration of the water/heavy water mixture should be slightly modified for studies as a function of temperature, but it is shown below that this does not modify the qualitative conclusion drawn from this study. The values the length scattering densities are given in Table 1.

Table 1.

chem structure	$10^{10}\rho$ (cm^{-2})
H_2O	−0.56
D_2O	6.38
H_2O/D_2O (82.4%/17.6%)	0.66
PEO	0.66
$-CH_2$	−0.31
$-CH_3$	−1.03
$-CD_2$	7.53
$-CD_3$	6.015
$-(CH_2)_{15}CH_3$	−0.382
$-(CD_2)_{17}CD_3$	7.39

Table 2.

sample	CAC (g mL^{-1})	N_{ag} (no. of polymer chains for CAC < C < C_f*)	C_f* (g mL^{-1})
M16C16	3×10^{-4}	34 ± 3	0.05
D32C16	1×10^{-3}	17 ± 2	0.02
D35CD18	2×10^{-4}	20 ± 2	0.015

Results Obtained at Room Temperature and Comparison with Theoretical Predictions

The three samples were already studied by different other methods, and some characteristic parameters are given in Table 2: CAC determined by fluorescence (using pyrene as probe); aggregation number, N_{ag}, estimated from static and dynamic light scattering and the concentration of "flower" or micelle overlap, C_f*, which is close to C_η at which the viscosity abruptly increases.[10,11]

The concentrations of the solutions ranged between 1 and 20% for M16C16 and D32C16 and between 1 and 35% for D35CD18. All the neutron scattering experiments were performed at $C >$ CAC and C_f*, except for the lower concentration studied which is close to C_f*.

(1) Studies in Water/Heavy Water (17.6%/82.4%, v/v)**.** In the mixture water/heavy water (17.6%/82.4%, v/v), scattering is only due to the micelles' cores. Only the semidilute system was investigated due to the relatively small amount of scattering species present in the solution. Generally, the scattering curves shown in Figures 6a−d exhibit a first peak followed by a shoulder at higher q values. The intensity ΔI_{max} increases linearly with concentration, and Figure 7 shows that for D35CD18 in water/heavy water (17.6%/82.4%, v/v) $\Delta I_{max}/C$ remains constant over a broad range of concentrations. The positions of the peaks (q_{max}) are shifted toward higher q values when concentration increases. By considering the first peak as a Bragg peak, the q_{max} value of the first peak gives an estimate of the average distance between the centers of micelles D:

$$D = \frac{2\pi}{q_{max}} \quad (29)$$

For micelle dispersions with constant aggregation number, D is expected to vary as C^{-a} (with $a = 1/3$) and q_{max} as $C^{1/3}$. Figure 8 shows that the exponent a is equal to 0.24, which is significantly lower than 1/3. This result, consistent with those previously found,[5,6] can be explained by an increase of aggregation number with increases in concentration. We have recently shown that the association mechanism of these polymers corresponds rather well to a model of closed association.[10,11] This model considers a given value of N_{ag} which depends on the lengths of PEO chain and aliphatic end groups. N_{ag} is expected to remain constant for CAC < C < C_f*

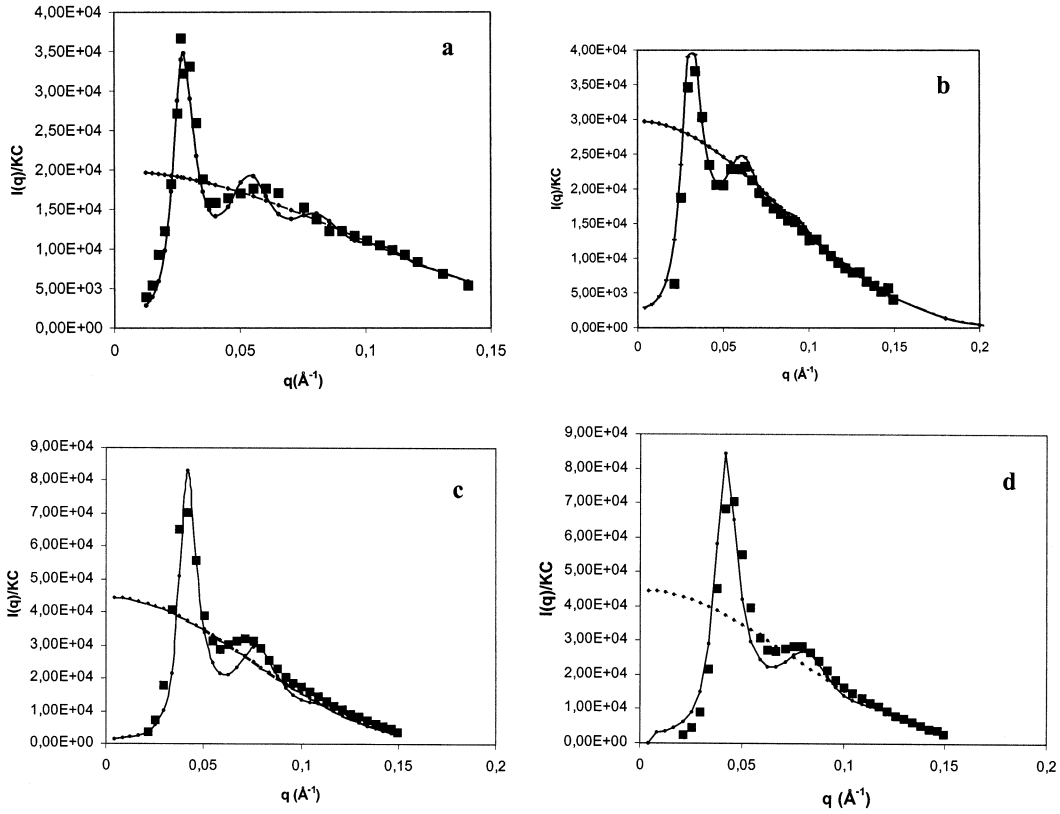

Figure 6. Experimental (■) and calculated (—) scattering intensities for the semidilute solutions of D35CD18 in water/heavy water (PEO matched) at four concentrations (5, 10, 35, and 50% for (a)−(d), respectively). The form factor of the core calculated according to eq 10 is indicated by the dotted line.

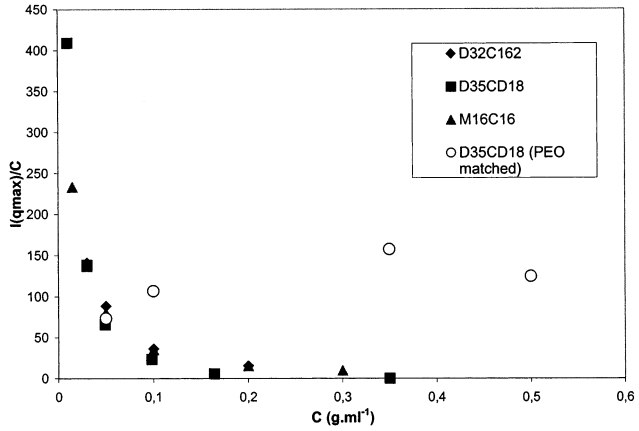

Figure 7. Magnitude of scattering peak reduced by the concentration against the concentration for M16C16, D32C16, and D35CD18 in heavy water and D35CD18 in the mixture water/heavy water (PEO matched).

(C_f* being the concentration at which micelles or flowers overlap), but it has been predicted that screening of the repulsive interactions in the micellar coronas above C_f* provokes an increase in N_{ag}.[44]

The scattering curves obtained with D35CD18 in the mixture D_2O/H_2O were fitted by eq 25. The results are shown in Figure 6. Equation 25 leads to goods fits and well predicts the peaks and shoulders observed. Moreover the high q ranges of the curves which correspond to the form factor alone are in reasonable agreement with a form factor for uniform spheres. This confirms previous analysis of analogous results obtained with other systems. In Table 3, the values of the three parameters of these fits, R_c, R_{hs}, and Φ, are shown.

Several observations can be made:

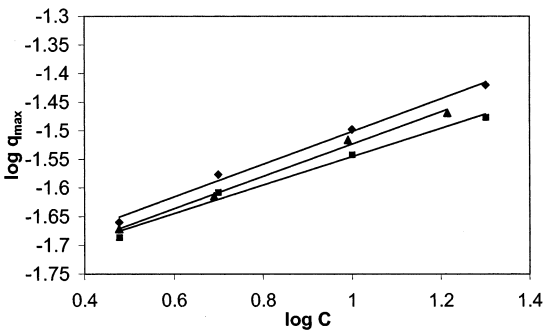

Figure 8. Position of the peak in the scattering intensity versus concentration in log−log scale for M16C16 (■), C32C16 (◆), and D35CD18 (▲).

Table 3.

concn (g mL^1)	0.05	0.1	0.35	0.5
vol fraction Φ	0.42	0.39	0.42	0.4
core radius R_c (nm)	1.67	1.90	2.20	2.20
aggregation no. N_{ag}	40	60	90	90
interaction radius R_{hs} (nm)	130	100	80	70

(i) The aggregation number found through this fit is not a constant but varies as approximately $C^{0.09}$. This result is quite consistent with the variation as $C^{-0.25}$ of the intermicellar distance instead of $C^{-0.33}$. This confirms the growth of the micelles with increasing C above C_f*.

(ii) The interaction radius R_{hs} decreases when concentration increases as $C^{-0.25}$.

(iii) The volume fraction is quite independent of concentration and always close to 0.4.

(iv) The two last points justify weak interpenetration of coronas at $C > C_f$*, which enables one to use the

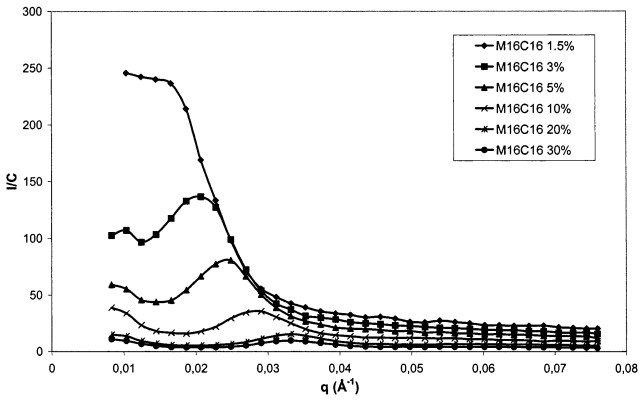

Figure 9. Scattered intensity for monofunctionalized PEO (M16C16) in heavy water, at different concentrations at room temperature. Lines are guides for the eye.

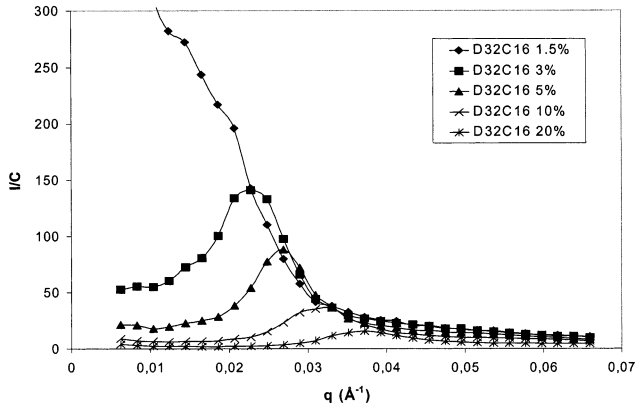

Figure 10. Scattered intensity for difunctionalized PEO (D32C16) in heavy water, at different concentrations at room temperature. Lines are guides for the eye.

model of effective hard spheres for the modeling of the intermicellar repulsion.

(2) Studies in Heavy Water (Core +Corona). In heavy water, we measured the scattering from the complete micelles (PEO chains + aliphatic end groups). Due to the very low weight fraction of end groups in these molecules, it is easy to show that the main contribution is that of PEO chains.

(a) Experimental Results. Figures 9 and 10 show the variations of ΔI versus q, for different polymer concentrations including dilute and semidilute regimes, for the polymers M16C16 and D32C16.

As already observed,[5,6] these curves are completely different from those obtained for semidilute solutions of nonmodified linear polymers and exhibit a shoulder (at lower concentrations) or a peak (at high concentrations) at q_{max}. q_{max} is shifted toward high q values when the concentration increases, as in the previous case. This behavior indicates the strong repulsion between the PEO micelle or "flower" corona, due to the fact that PEO is in good solvent at this temperature. Figure 8 shows that the exponent a is equal to 0.24 and 0.29 for M16C16 and D32C16, respectively, and is close to that obtained for D35CD18. This confirms the increase of aggregation number with increases in concentration.

As seen in Figures 7, 9, and 10, the intensity at the top of the peak ΔI_{max} passes through a maximum when concentration increases. In Figure 7, we have presented the variation of $\Delta I_{max}/C$ versus C for M16C16, D32C16, and D35CD18 in heavy water. Similar behaviors are observed in the three cases with ΔI_{max} tending to zero

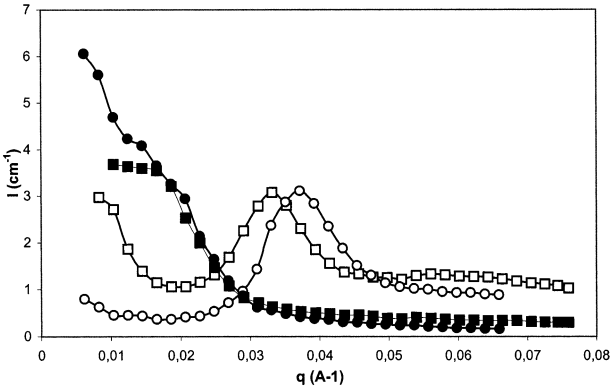

Figure 11. Scattered intensity for monofunctionalized PEO (squares) and difunctionalized PEO (circles) at 1.5% (full symbols) and 20% (open symbols). Lines are guides for the eye.

for $C > 0.15$ g mL^{-1}. This does not indicate a disappearance of the solution order, but in agreement with the theoretical predictions, this phenomenon is due to the overlapping of micelles or flowers and for $C \gg C_f^*$, a behavior close to that described for a semidilute solution of polymer is expected.

As M16C16 and D32C16 have the same hydrophobic/hydrophilic balance, it is interesting to compare the obtained scattering curves for each at the same concentration (Figure 11). At lower concentrations, 0.015 g mL^{-1}, the excess scattered intensity at small q is much higher for D32C16 than for M16C16. We could attribute this difference to the presence of solution heterogeneities (aggregates) for D32C16. We have already shown by light scattering that in this range of concentration, above CAC but below C_f^*, the formation of bridges is necessarily associated with the formation of flower aggregates.[10,11] For the higher concentration 0.2 g mL^{-1}, the curves of D32C16 and M16C16 are not superimposed and a shift to high q value is observed for D32C16 with respect to M16C16. This suggests that the aggregation number of D32C16 is lower than that of M16C16. Moreover in the higher q range, a shoulder appears for M16C16 and is absent for D32C16.

(b) Comparison with Theoretical Predictions. (i) Dilute Regime $C < C_f^*$. The calculated and experimental curves obtained with the monofunctionalized sample M16C16 at $C_1 = 0.015$ g mL^{-1} are compared in Figures 12a. From previous measurements on the same polymer, one can conclude that $C_1 < C_f^*$. Indeed, from static light scattering and neutron data, a value of 34 was found for N_{ag} and dynamic light scattering has provided a value of the hydrodynamic radius R_H of 15.5 nm. By using for C_f^*

$$C_f^* = \frac{\overline{M_w} N_{ag}}{\frac{4}{3}\pi N_A R_H^3} \tag{30}$$

one finds $C_f^* = 0.05$ g mL^{-1}, a value much higher than C_1. The form factor calculated from eq 14 is presented in the insert of Figure 12a. Even in the high q range, where $S(q)$ is expected to be close to 1, the fit of the experimental results is poor. This shows that it is necessary to take into account correlated fluctuations of the monomer density inside the micellar coronas (second term of eq 11). Figure 12a shows that eq 11 fits reasonably well the experimental $\Delta I(q)$ values. The value of N_{ag} introduced in the calculations was 34, as

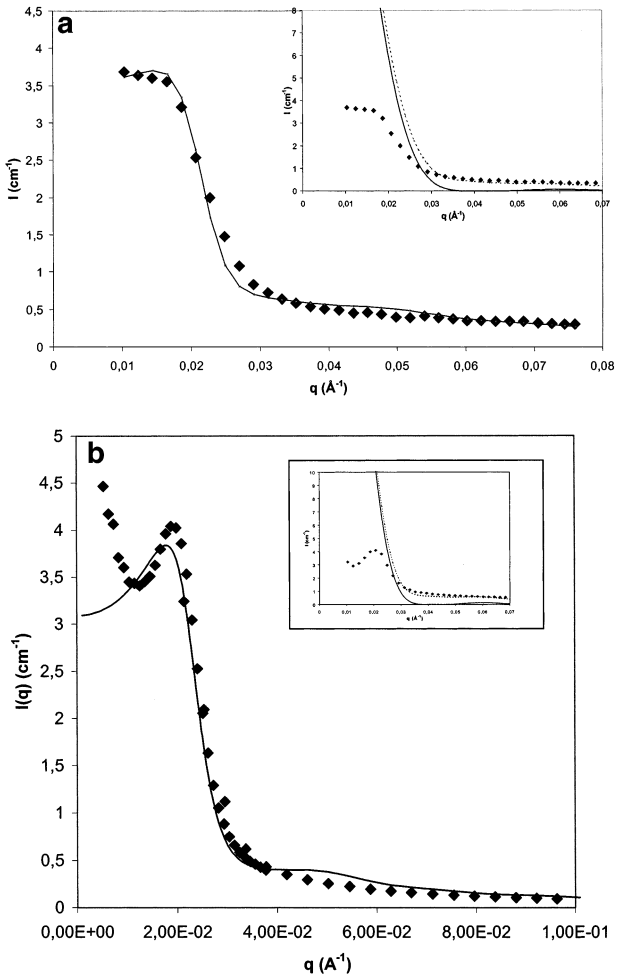

Figure 12. Comparison between experimental results for M16C16 (1.5%) (a) and D35CD18 (1%) (b) (◆) and theoretical calculations according to eq 11. (−) Full eq 11 with $S(q)$ calculated from eq 5. Insert: $S(q) = 1$; without (◆) and with (···) taking into account the local fluctuations of polymer density in the corona (second term in eq 11).

previously obtained, and the value of the volume fraction was deduced from N_{ag} using eq 8. The best fit (Figure 12a) in the whole range of q was obtained using $R = 18$ nm (form factor) and $R_{hs} = 14$ nm (structure factor), values close to that of the hydrodynamic radius $R_H = 15.5$ nm.

Our previous light scattering experiments have shown that the aggregation number of D32C16 flowers for $C < C_f^*$ corresponds to 17 molecules of $M_w = 32\,000$ g mol^{-1} or 34 "half" molecules of $M_w = 16\,000$ g mol^{-1}. The simple form factor of star, $P(q)$, does not give so good a description of the high q ranges of the curves as the corrected $P(q)$ function (eq 11) as for M16C16 (Figure 12b). Besides, the calculated ΔI function well fits the whole scattering curve.

Hence, in the dilute regime, the scattering behavior of the micellar solution is consistent with a model using a form factor of polymer stars supplemented by the term reflecting the density fluctuations inside the micelles and a structure factor for hard spheres, the interaction radii being close to the micelle radii.

(ii) Semidilute Regime. In Figure 13, the fits obtained by using eq 24 for the difunctionalized sample D32C16 at two concentrations (0.1 and 0.2 g mL^{-1}) are shown. Initially, we calculated the value of ρ using the theoretical eqs 15−17. This corresponds to 4.8 and 3 nm for 0.1 and 0.2 g mL^{-1} dispersions, respectively. These values do not give a good fit for the experimental curves. Then we kept ρ and R_{hs} as adjustable parameters and obtained the results presented in Figure 13. The following parameters were drawn from these fits:

$$C = 0.1 \text{ g mL}^{-1},\ \rho = 6.0 \text{ nm and } R_{hs} = 9.5 \text{ nm};$$

$$C = 0.2 \text{ g mL}^{-1},\ \rho = 4.8 \text{ nm and } R_{hs} = 7.7 \text{ nm}.$$

The value of R_{hs} at $C = 0.1$ g mL^{-1} is very close to that found for sample D32CD18 in the mixture H_2O/D_2O, $R_{hs} = 10$ nm, D32C16 and D35CD18 being samples of similar hydrophobic/hydrophilic balance.

The fact that the values of ρ are higher than those calculated directly from eqs 15−17 may be due to the fact that we used a star model under Θ conditions even while the radius of micelles, R, was the true radius measured by light scattering. In fact, at room temperature water is a rather good solvent for PEO. The value of R_{hs} is much higher than ρ. This indicates weak interpenetration of the micellar coronas at concentrations slightly exceeding the overlap concentration C^*. Therefore, a simple model of effective hard spheres can lead to good fit for the structure factor of the solution of micelles at higher concentrations. At a higher degree of overlap, the radius of noninterpenetrated internal regions of the corona could be considered as an effective interaction radius. The volume fraction of interacting micelles Φ calculated from the values of R_{hs} providing the best fit is virtually independent of polymer concentration (0.39 and 0.42 for 0.1 and 0.2 g mL^{-1},respectively). This may be attributed to a compensation of the effect of increase of the number of micelles which should tend to increase Φ and the overlap of the micelles, which leads to stronger interpenetration of the coronas.

It must be noted that, in our calculations, we have not taken into account either the wavelength spread of the neutron beam or the micelle polydispersity.

(3) Temperature Effects. It is well-known that the aqueous PEO solutions exhibit phase diagrams characterized by a lower critical solution temperature, LCST,[45] phase separation occurring with increasing temperature and for a PEO with an infinite molecular weight the Θ point is 100 °C. This means that the solvent quality of water decreases and as consequence the radius of gyration of a PEO chain decreases with heating. The evolution of the scattering intensity versus temperature should constitute a qualitative check of our theoretical approach. An increase of temperature is expected to increase the scattered intensity at the peak due to decreasing interpenetration of the coronas, when PEO chains are not matched. A different behavior should be observed when PEO is matched.

Figure 14 allows the comparison of the evolution of scattering curves for the same polymer (D35CD18 at 0.35 g mL^{-1} that is larger than C^*) in heavy water or in the mixture water/heavy water (17.6%/82.4%, v/v). Figure 14a shows that a peak absent in heavy water at 25 °C reappears at 53 and 72 °C. The inverse behavior is obtained in the solvent mixture: ΔI_{max} decreases upon increasing T, and moreover, the second peak, which is well pronounced at 25 °C, appears only as a shoulder at 53 and 72 °C. This result is in agreement with previous observations for a PEOM of lower molecular weight (4000 g mol^{-1}) with two end groups of 12 carbons; the X-ray scattering curves exhibit up to 6

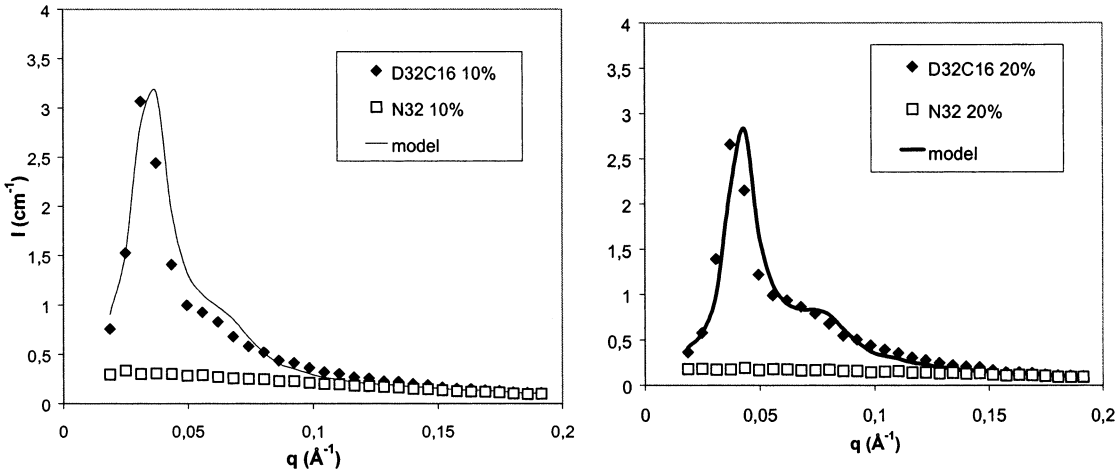

Figure 13. Experimental (◆) and calculated (−) scattering intensity for the semidilute solutions of D32C16 and N32 in heavy water at two concentrations (10 and 20%).

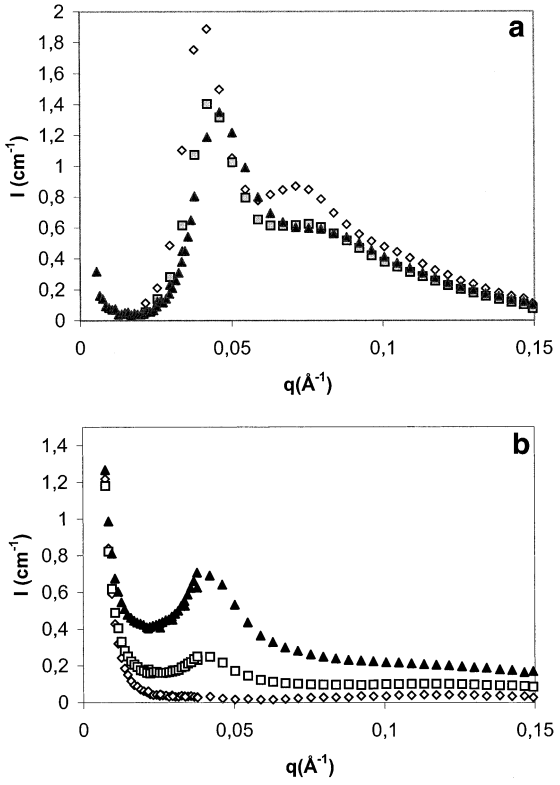

Figure 14. Evolution of the scattering curves (ΔI versus q) with temperature for D35CD18 at 35% in heavy water (a) and in a mixture of water/heavy water (PEO matched) (b).

narrow peaks at room temperature, and at $T > 45$ °C, only two broader peaks are observed.[7] For such systems, order−disorder transitions occur with heating, a behavior completely different from that observed with ethylene oxide/propylene oxide, EO/PO, associative copolymers. It becomes obvious that the reappearance of a peak in Figure 14a is not related to a better organization in the system but simply to a smaller degree of overlap of the PEO corona of the micelles.

Remark: We have not considered the variation of molar volume of PEO, V_{PEO}, with temperature. In heavy water, an increase of V_{PEO} of less than 10% is expected in the range of temperature 25−70 °C. The increase of scattered intensity in much higher than 20%. In the case of solvent mixture, the change in V_{PEO} should induce a poorer matching conditions (at 70 °C, the good matching

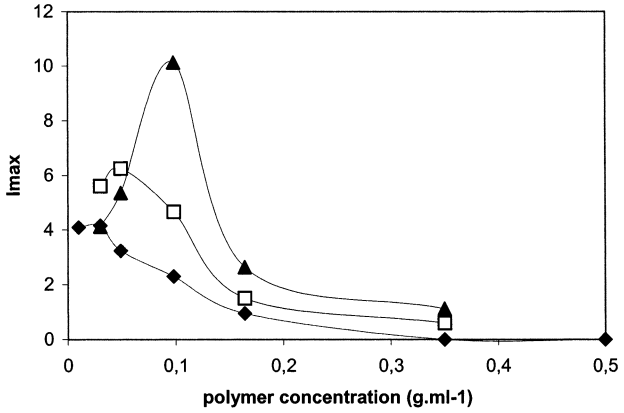

Figure 15. Variation of the magnitude of the peak in the scattering intensity versus concentration for D35CD18 at three different temperatures 25 °C (◆), 53 °C (□), and 72 °C (▲). Lines are guides for the eye.

mixture should be approximately water/heavy water 18.4/81.6% v/v). The contribution of the PEO chains should become more important, and the scattered intensity should increase and not decrease. One can conclude that the evolutions of the spectra with temperature are really due to changes in physical behaviors.

The evolution of scattering curves with temperature was also studied at various concentrations for D35CD18 (10%) in heavy water. In Figure 15, I_{max} is plotted versus concentration at three different temperatures. All the curves exhibit a maximum at a concentration which increases when temperature increases. This maximum, which roughly corresponds to the flower overlap, is shifted toward higher values with increments in temperature. Qualitatively speaking, two effects can be taken into account: (i) There is decreasing repulsion between PEO chains, and therefore, the aggregation number of micelles is expected to increase. (ii) The corona radii decrease due to the loss of solvent quality. Since $C^* \propto (\overline{M_w} N_{ag})/R_{gs}^3$, C^* should be an increasing function of temperature as observed in Figure 15.

Conclusion

This work presents neutron scattering studies of solutions of hydrophobically end-capped poly(ethylene oxide) which self-associates to form micelles or "flowers" (in the case of one or two hydrophobically modified ends, respectively) and an attempt to model the resulting

scattering curves. The observed scattering behavior is consistent with that predicted theoretically on the basis of analogy between the structure of the micellar solution and the solutions of starlike polymers.

In the dilute regime the structure factor of the micellar solution reflects repulsive steric interactions between coronas of the micelles swollen in a good solvent. These repulsive interactions can be mimicked by the hard sphere potential with an effective interaction radius which is close to the hydrodynamic radius of micelles. Together with the form-factor calculated by taking into account the power-law radial dependence of the polymer density in the micellar corona, the equivalent hard sphere structure factor provides a good fit of the experimental data.

The analysis of the scattering curves obtained in the semidilute regime (above the overlap concentration of micelles) for both one-and two-end-modified polymers indicates that (i) micelles are organized in a liquidlike ordered structure and (ii) the effective interaction radius scales with concentration as the distance between centers of the micelles. Altogether this confirms weak interpenetration of the coronas of micelles in a wide range of concentration, corresponding to semidilute solution. Our data confirm an increase in the aggregation number upon an increase in concentration, which is expected due to partial screening of the repulsive interactions in the coronas. A decrease in the magnitude of the interaction peak in the scattering intensity upon an increase in concentration is explained by an increase of the relative contribution of local fluctuations of the polymer density (similar to that in semidilute solutions of linear chains) to the overall scattering and, correspondingly, decrease in the relative contribution of correlated fluctuations in the positions of micelles.

The latter observation is consistent with the effect of increasing temperature (decreasing solvent strength) on the scattering curves: partial collapse of the micellar coronas due to decreasing solvent strength leads to the shift of the overlap concentration and, therefore, to the decrease in the degree of overlap of micelles at a given concentration (exceeding C^*). Therefore, the scattering peak disappears with increasing temperature provided the micellar coronas are not matched, while the opposite effect is observed in case of matched coronas.

The behavior of the micellar solution is the same for mono- and difunctionalized polymers with the same hydrophilic hydrophobic balance. The shift of the interaction peak position to higher q values in a semidilute solution of difunctionalized chains may indicate the contribution of the bridging attraction to the interaction between the micelles.

Acknowledgment. The authors acknowledge insightful discussions with M. Daoud and P. Guenoun.

References and Notes

(1) *Polymers in Aqueous Media, Performances through Association*; Glass, J. E., Ed.; Advances in Chemistry Series 223; American Chemical Society: Washington, DC, 1989.
(2) *Hydrophilic Polymers, Performances and Environmental Acceptability*; Glass, J. E., Ed.; Advances in Chemistry Series 248; American Chemical Society: Washington, DC, 1995.
(3) Lundberg, D.; Glass, E.; Eley, R. R. *J. Rheol.* **1991**, *35*, 1255.
(4) Yekta, A.; Xu, B.; Duhamel, J.; Adiwidjaja, H.; Winnik, M. A. *Macromolecules* **1995**, *28*, 956.
(5) François, J.; Maitre, S.; Rawiso , M; Sarazin, D.; Beinert, G.; Isel, F. *Colloids Surf.* **1996**, *112*, 251.
(6) Alami, E.; Rawiso, M.; Ise, F.; Beinert, G.; Binana-limbele, W.; François, J. In *Hydrophilic Polymers, Performance with Environmental Acceptability*; Glass, J. E., Ed.; Advances in Chemistry Series 248; American Chemical Society: Washington, DC, 1995; p 343.
(7) Abrahmsen-Alami, S.; Alami, E.; François, J. *J. Colloid Interface Sci.* **1996**, *179*, 20.
(8) Alami, E.; Almgren, M.; Brown, W.; François, J. *Macromolecules* **1996**, *29*, 2229.
(9) Chassenieux, C.; Nicolai, T.; Durand, D. *Macromolecules* **1997**, *30*, 4952.
(10) Gourier, C.; Beaudoin, E.; Duval, M.; Sarazin, D.; Maître, S.; François, J. *J. Colloid Interface. Sci.* **2000**, *230*, 41.
(11) Mortensen, K. *J. Phys. Condens. Matter* **1996**, *8*, 103.
(12) Mortensen, K.; Brown, W. *Macromolecules* **1993**, *26*, 4128.
(13) Mortensen, K.; Brown, W. *Macromolecules* **1994**, *27*, 5654.
(14) Mortensen, K.; Pedersen, J. S. *Macromolecules* **1996**, *29*, 805.
(15) Richter, D.; Jucknischke, O.; Willner, L.; Fetters, L. J.; Lin, M.; Huang, J. S.; Roovers, J. E. L.; Toporowski, P. M..; Zhou, L. L. *J. Phys. IV* **1993**, *3*, 3.
(16) Pedersen, J. S.; Gerstenberg, M. C. *Macromolecules* **1996**, *29*, 1363.
(17) Perreur, C.; Habas, J. P.; François, J.; Lapp, A.; Peyrelasse, J. To be published.
(18) Benoit H. *C. R. Acad. Sci.* **1955**, 533.
(19) Benoit H. *J. Polym. Sci.* **1953**, *11*, 507.
(20) Benoit, H.; Joanny, J. F.; Hadziiannou, G.; Hammouda, B.; *Macromolecules* **1993**, *26*, 5790.
(21) Forster, S; Burger, C. *Macromolecules* **1998**, *31*, 879.
(22) Cogan, K. A.; Gast A. P.; Butun V.; Armes S. P. *Macromolecules* **1999**, *32*, 4302.
(23) Cogan, K. A.; Gast, A. P.; Capel, M. *Macromolecules* **1991**, *24*, 6512.
(24) Stellbrink, J.; Willner, L.; Richter, D.; Lindner, P.; Fetters, L. J.; Huang, J. S. *Macromolecules* **1999**, *32*, 5321.
(25) Toporowski, P. M.; Roovers, J. E. L. *Macromolecules* **1978**, *11*, 365.
(26) Kirste, R. G.; Oberthur, R. C. In *Small-Angle X-ray Scattering*; Glatter, O., Kratky, O., Eds.; Academic Press: New York, 1982; p 387.
(27) Witten T. A.; Pincus P. A. *Macromolecules* **1986**, *19*, 2509.
(28) Likos, C. N.; Löwen, H.; Watzlawek, M.; Abbas, B.; Jucknischke, O.; Allgaier, J.; Richter, D. *Phys Rev. Lett.* **1998**, *80*, 4450.
(29) Gast A. P. *Langmuir* **1996**, *12*, 4060.
(30) Higgins, J. S.; Benoit, H. C. *Polymers and Neutron Scattering*; Clarendon Press: Oxford, U.K., 1994.
(31) Auvray, L. *Acad. Sci. (Paris)* **1986**, *302 II*, 859. Auvray, L.; de Gennes, P. G. *Europhys. Lett.* **1986**, *2*, 647.
(32) Muller, F.; Delsanti, M.; Auvray, L.; Yang, J.; Chen, Y. J.; Mays, J. W.; Deme, B.; Tirrel, M.; Guenoun, P. *Eur. Phys. J. E* **2000**, *3*, 45.
(33) Forster, S.; Hermsdorf, N.; Leube, W.; Schnablegger, H.; Regenbrecht, M.; Akarai, S.; Lindner, P.; Boettcher, C. *J. Phys. Chem.* **1999**, *103*, 6657.
(34) Pedersen, J. S. *J. Chem. Phys.* **2001**, *114*, 2839.
(35) Beaudoin, E. Ph.D. Thesis, Université de Pau et des Pays de l'Adour, 2001.
(36) Daoud, M.; Cotton J. P. *J. Phys. (Paris)* **1982**, *43*, 531.
(37) Zhulina, E. B. *Vysokomol. Soedin. B* **1983**, *25*, 834; *Vysokomol. Soedin. A* **1984**, *26*, 794. Birshtein, T. M.; Zhulina, E. B. *Polymer* **1984**, *25*, 1453.
(38) Wijmans, C. M.; Zhulina, E. B. *Macromolecules* **1993**, *26*, 7214.
(39) Birshtein, T. M.; Zhulina, E. B.; Borisov, O. V. *Polymer* **1986**, *27*, 1078.
(40) Marques, C. M.; Izzo, D.; Charitat, T.; Mendes, E. *Eur. Phys. J. B* **1998**, *3*, 353.
(41) Broseta, D.; Leibler, L.; Lapp, A.; Strazielle, C *Europhys. Lett.* **1986**, *2*, 733.
(42) Kaczmarski, J. P.; Glass J. E. *Macromolecules* **1993**, *26*, 5149.
(43) Maitre, S. Ph.D. Thesis, University Louis Pasteur, Strasbourg, France, 1997.
(44) Birshtein, T. M.; Zhulina, E. B. *Polymer* **1989**, *30*, 170.
(45) Saeki, S.; Kuhawara, N.; Nakata, N.; Kanako, N. *Polymer* **1976**, *17*, 685.

MA011027L